

In vivo implant mechanics of single-shaft microelectrodes in peripheral nervous tissue

Winnie Jensen¹, Ken Yoshida^{1,3} and Ulrich G. Hofmann²

Abstract— The VSAMUEL consortium developed silicon-based, electrode arrays (referred to as *ACREO* electrodes), that may one day provide a highly selective neural interface for neuroscience or neural prosthesis applications. We previously reported on the successful insertion into brain tissue. In the present work, we investigated the feasibility of implanting the *ACREO* electrodes into peripheral nerve. We compared the implant mechanics of single shaft silicon *ACREO* electrodes (25 x 38 x 15000 µm) and conventional tungsten needle electrodes (50µm diameter). Experimentally measured implant forces were measured *in vivo* (1 acute rabbit, 2 mm depth, 2 mm/s velocity). The force required for the tungsten electrode to first penetrate the perineurium was in average 7.4 ± 3.9 mN, whereas the maximum force the electrode had to withstand during the entire insertion/retraction was 11.3 ± 2.8 mN. It was not possible to facilitate perpendicular insertion of the *ACREO* electrode without breaking it. The critical buckling force of the *ACREO* electrode was theoretically estimated to 1–4 mN, which proved consistent with the experimentally measured break force (5.1 ± 2.1 mN). Bending moment analysis showed that tungsten could withstand ultimate stresses 4–10 times higher than our silicon-based electrodes. Before the *ACREO* electrodes can be safely used for peripheral and spinal cord implants we recommend to shorten and thicken the probes to increase their mechanically strength.

Keywords— peripheral nerve, electrode, implant mechanics

I. INTRODUCTION

An essential part in the future success of neural prosthesis applications is the availability of reliable and highly selective neural interfaces, such as the silicon-based micro electrode arrays recently developed by VSAMUEL consortium (EU FP6, IST-1999-10073) [1-4]. The silicon electrode arrays designed by the VSAMUEL consortium were manufactured at ACREO AB, Kista, Sweden and consisted of up to 64 channels distributed on 1-8 shafts [2], and will therefore be referred to as the *ACREO* electrodes in the present work. We have previously reported on the electrical [5] and mechanical [6;7] properties of the *ACREO* electrodes, and on the feasibility of using the electrodes as intra-cortical implants in basic neuroscience research [8-10]. The focus of the present work was to further report on ongoing mechanical evaluation.

¹Dept. Health Science and Technology, Aalborg University, Denmark (e-mail: wj@hst.aau.dk). ²Universität zu Lübeck, Institut für Signalverarbeitung und Prozessrechentechnik, Lübeck, Germany (e-mail: hofmann@isip.uni-luebeck.de). ³Biomedical Engineering Dept, Indiana University-Purdue University Indianapolis, U.S.A. (e-mail: yoshidak@iupui.edu).

The mechanical behavior of an electrode during implantation into neural tissue can have a profound effect on the neural connections and signaling that takes place within the tissue [11]. The type of insertion method and the mechanical impact on the nerve is highly different for the individual peripheral nerve interfaces mentioned above. The cuff electrode is the least invasive type of implantable electrodes, since it is placed around the intact nerve trunk and held in place by attaching the lead wires to the surrounding tissue. Other types penetrate the perineurium and thereby place the recording sites within the nerve trunk in closer proximity with the individual axons.

The mechanical impact of inserting micro-electrodes [6;7;11-14]] or surgical probes [15;16] into brain tissue has been studied. However, to the best of the authors' knowledge, there are no previous studies on the *in vivo* insertion mechanics of electrodes being implanted into peripheral nerve tissue. The objective of the present work was to examine the feasibility of *in vivo* implantation of the *ACREO* microelectrodes in peripheral nervous tissue. We compared the *in vivo* implant mechanics of the flexible, silicon-based *ACREO* microelectrodes and conventional, commercially available tungsten electrodes, and the analysis included analysis of *in vivo* insertions and retractions in rabbit peripheral nerve and theoretical calculations to estimate the failure mode of the two types of electrodes. In the present paper we report on *in vivo* peripheral nerve insertion force data obtained with a novel tension-compression force measurement technique. Our results may form a better base for electrode design and development of implant techniques for the future.

II. METHODS

A. Description of electrodes

The single shaft silicon electrode had a cross sectional area of 25 x 38 µm at the electrode site, and the area expanded to 25 x 200 µm at the shaft base. Each of the shafts carried a number of 10 x 10 µm Pt-Ir sites and had a tip opening angle of 4°. The specific details of the electrode and manufacturing processes are described in detail in [4]. The *ACREO* electrodes were compared to commercially available, round tungsten rods (no insulation, 50 µm diameter, A-M Systems). The rods were cut into appropriate lengths and then manually electro-sharpened to create a sharp tip. The tips were visually inspected through a microscope after the electrolyses process, and the resulting opening angle was measured. All electrodes were cleaned in de-ionized water before implantation.

B. Experimental procedures

Approval was obtained from the Danish Committee for the Ethical Use of Animals in Research. Data was collected from one New Zealand White rabbit placed under general anaesthesia (IM injections of 0.15 mg/kg Midazolam (Dormicum™, Alpharma A/S, Norway), 0.03 mg/kg Fentanyl and 1 mg/kg Fluranison). The sciatic nerve and its distal tibial and peroneal branches were exposed in the rabbit's left leg to provide sufficient space for the implantation experiments. At the end of the experiment euthanasia was induced by an overdose injection of sodium pentobarbital.

Simultaneous recordings were made of tension and compression forces and the distance traveled by the microelectrode during repeated penetration and retraction of the electrodes into peripheral nerve (ramp-and-hold profile, velocity 2 mm/s, excursion 2 mm). The insertion sequence was repeated twice at each position, such that the first insertion reflect the penetration force with the perineurium intact, and the second insertion characterize the forces necessary to advance the electrode through the endoneurium. The force was measured using a load cell (Sensotec Inc. model 31/1435-02, resolution calibrated to 1.31 mV/g). The electrodes were advanced into the tissue using a computer-controlled hydraulic micromanipulator (Narishige MMO-220, Maxon Motor 22-60-881). A position resolution of ~0.25 μm was thereby achieved. The force signal was low pass filtered before sampling (2.5 kHz, NI DAQCard-6204E). The sampled data were filtered offline (3rd order Butterworth at 10 Hz), and linear drift was removed. Statistical evaluation of the force at the selected points was performed (ANOVA analysis, Turkey-Kramer post-hoc evaluation, p<0.05).

Pilot studies demonstrated that direct, perpendicular insertion of electrodes into the peripheral nerve was not possible, i.e. the peripheral nerve would simply yield under the advancing electrode or the electrode would slide off the nerve trunk surface. We therefore chose to mechanically stabilize the peripheral nerve trunk by adding support underneath, since it was the fastest, easiest and least invasive method.

C. Theoretical buckling analysis

The structural mechanics of single-shaft *ACREO* and tungsten electrodes were analyzed to estimate their ultimate failure mode (i.e. breaking). Buckling of homogenous materials in compression can be described by Euler's equation. Both free-fixed and pin-fixed buckling were visually observed during the in-vivo peripheral insertion experiments, so these two models were therefore included in the buckling force analysis, see Figure 1. In the case of the tungsten electrodes, only pin-fixed buckling mode was observed. A relationship predicting the critical buckling force as a function of the length was then derived from Euler's equation and the critical buckling forces calculated. The geometry of the needle was modeled as a cylinder of fixed radius (50 μm diameter), which is a relatively good approximation of the shape of the needle except for its very tip, where the equations will overestimate the critical buckling force. In the case of the *ACREO* electrode the

thickness of the substrate remains constant, however, the width of the electrode varies depending upon the distance from the tip. Since the equations used to estimate the critical buckling force only describe a uniform cross section beam, the electrode shaft was modeled as a beam of constant width at that particular distance from the tip. This provides an estimate of the critical buckling force, since the beam under analysis has a wider cross section than the actual electrode. The values that were used to calculate the critical buckling force were as follows. Young's elastic modulus for silicon = 190 GPa, Young's elastic modulus for tungsten = 400 GPa and centroidal moment of inertia for tungsten = $0.31 \times 10^{-18} \text{ m}^4$. The value of the effective length was varied in the analysis.

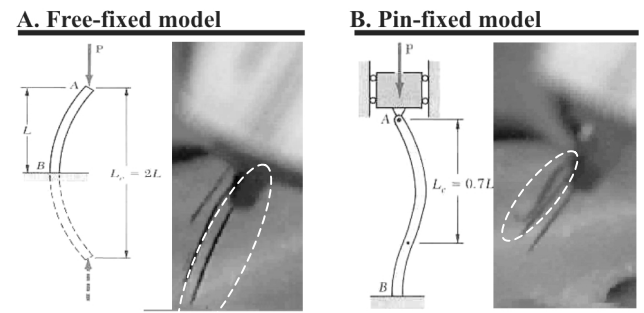


Figure 1. A) Example of free-fixed buckling (circled left). One tip is free to translate laterally (effective length = $2L$). B) Example of pin-fixed buckling (circled right). The electrode tip is not allowed to translate laterally but can pivot (effective length = $0.7L$). L = shaft length.

D. Theoretical bending moment analysis

A bending moment analysis was conducted to determine and compare the quantitative estimates of the bending forces study in order to provide future design recommendations. The estimated bending forces, F_u , were calculated as a function of electrode length shown according to the following equation:

$$F_u = \frac{\sigma_u I}{cL}$$

In the equation, σ_u is the ultimate compressive strength of the material (silicon $\sigma_u=200\text{ MPa}$, tungsten $\sigma_u=600\text{ MPa}$). I is the minimum centroidal moment of inertia (was varied with the length for the *ACREO* electrode, while I was fixed at $0.31 \times 10^{-18} \text{ m}^4$ for the tungsten electrode. C is the maximum distance from the neutral axis, which was assumed to be half the substrate thickness. L is the length of the electrode (was varied in the analysis). For the *ACREO* electrodes it was assumed that the shaft had a constant cross sectional area. Further, no stress concentration factors were taken into consideration in either case, since it was assumed that the weakest plane of the electrodes was orthogonal to the changes in thickness.

III. RESULTS

A. Insertion force measurements

It was not possible to obtain perpendicular penetration of the *ACREO* electrodes into the peripheral nerve. In total, 22 attempted insertions using 6 different single-shaft electrodes were made. All electrodes buckled during the insertion attempt and eventually broke. It was possible to penetrate the perineurium with the tungsten electrodes when the nerve trunk was stabilized by the added support beneath. A typical example set of measured force and length data for a Tungsten electrode is shown in Figure 2. In total, data from 23 successful penetrations from 4 different tungsten electrodes were analyzed. We defined the compressive force as positive and tensile force as negative.

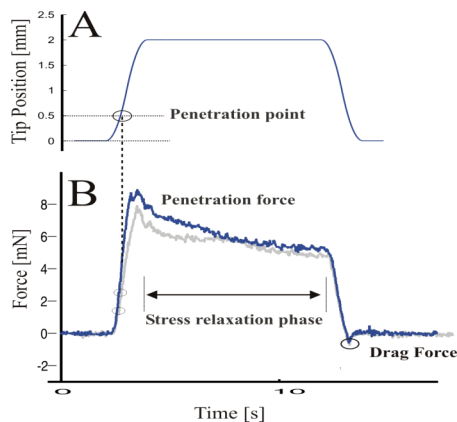


Figure 2. Typical force and length measurements of a tungsten electrode (dark grey curves = 1st insertion, light grey curves = 2nd insertion). A) Position of the electrode while advancing it into the peripheral nerve tissue. B) Corresponding force traces. We compared the penetration, maximum and drag forces.

We observed a continuous increase in the force until the **point of penetration** (defined as the first peak or reversal of force during insertion in the length/force curve). The average penetration force was 7.44 ± 3.94 mN (1st insertion) and 4.72 ± 3.02 mN (2nd insertion). The much smaller penetration force during the 2nd insertion indicates that the first penetration made a hole in the perineurium however there was no statistical difference among the data.

The **maximum compression force** is an estimate of the force that an electrode experiences during the entire procedure. This force was found to be 11.33 ± 2.79 mN (1st insertion) and 9.79 ± 2.26 mN (2nd insertion).

The **maximal tension force** experienced by the electrode during the retraction phase was -1.31 ± 0.86 mN (1st insertion) and -1.67 ± 0.61 mN (2nd insertion). The maximum tension force is almost a magnitude lower than the maximum compressive force which indicates, that the retraction phase will not have a significant mechanical impact on the electrodes.

B. Buckling analysis

The critical buckling force was calculated as function of the length and width of the electrode types and the results of the critical buckling force calculations are

given in Figure 3. The critical buckling force decreased with increasing electrode width and length for all models. At maximum electrode length, the critical buckling force for the single-shaft *ACREO* electrodes in pin-fixed buckling was predicted to be ~ 4 mN, while the free-fixed buckling model estimated a critical buckling force at ~ 1 mN (see Figure 3A). These measurements were consistent with the experimentally measured break forces (5.1 ± 2.1 mN, see Figure 3B).

The theoretical and estimated break force of the *ACREO* electrodes is approximately equal to the mean penetration force (4.72 ± 3.02 mN, 2nd insertion), which indicates that the *ACREO* might penetrate the perineurium without breaking, but only if a hole has already been opened in the connective tissue sheath. However, the break force is only about half of the maximal force experienced by the tungsten electrodes (9.79 ± 2.26 mN, 2nd insertion), which indicates that the *ACREO* electrodes cannot be expected to survive insertion into peripheral nerve in their current design.

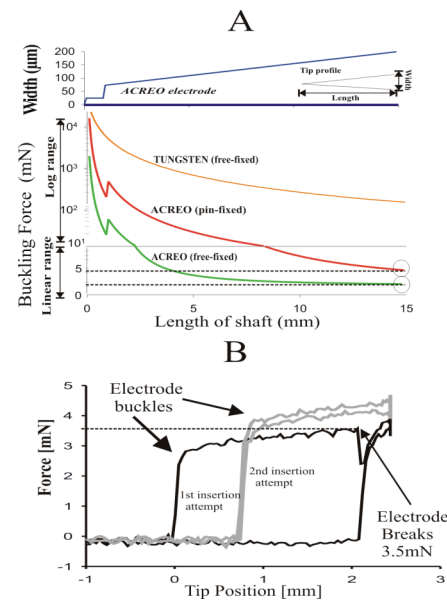


Figure 3. A) Calculation of critical buckling force as a function of electrode length (bottom plot). The change in width of the *ACREO* electrode as the length of the shaft increases (top plot). Note that the y-axis is a combination of log and linear scale. B) Experimentally measured stress-strain curves of the *ACREO* electrode advanced towards peripheral nerve tissue. No specific penetration points were observed.

C. Bending moment analysis

The result of the theoretical bending moment analysis is depicted in Figure 4. The cross-sectional, centroidal moment of inertia was found to play the largest role in the strength of the electrode, such that the wider the electrode is, the greater bending moment it can withstand. Although the ability of the electrode to withstand bending forces placed at its end is also proportional to the width of the structure, its effect is dominated by the moment arm acting generating the moment. The longer the electrode is, the weaker it becomes. The effect of the bulk material property is illustrated by the ultimate bending force curve for a tungsten rod of

approximately similar size as the *ACREO* electrode. Since tungsten has an ultimate stress between 4 – 10 times higher than silicon, it is mechanically 3 – 10 times more resistant to mechanical failure.

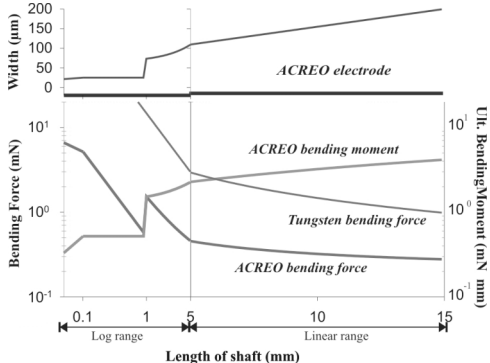


Figure 4. Calculation of the ultimate bending force and moment as a function of the length of the shaft. The two top plots show the change of the width of the *ACREO* electrode as the length of the shaft increases (the thickness is constant). Note the combination of log and linear scales in the plots.

IV. DISCUSSION AND CONCLUSIONS

We have previously reported on insertion force measurements [6], where the force was estimated by a linear displacement transducer using Hooke's law. In the present work, we used a method to assess the force with a high-resolution load cell. One clear advantage of this technique is the possibility to obtain data from both the implantation (compression force) and the retraction phases (tension force). We tested several methods to provide insertion of the *ACREO* electrode.

The only method that proved successful was indirect, parallel insertion by pulling the *ACREO* electrode through the nerve trunk (i.e. a 12 μ m fiber was glued to the tip of the electrode and a bigger needle was used to pull the electrode through). However, this manual method did not allow for simultaneous force measurements.

The penetration force for the tungsten needle was measured in the range 4.7 ± 3.0 mN to 7.4 ± 3.9 mN and the maximum force measured were in the range of 11.3 ± 2.8 mN to 9.8 ± 2.3 mN. In previous insertion force measurements in rat cerebral cortex tissue we found a maximal penetration force of the *ACREO* electrodes in the range of 2.4 ± 0.8 mN (5 parallel shafts) and 2.0 ± 0.8 mN (8 parallel shafts) [6;7]. The force that an electrode experience during peripheral nerve insertion is therefore an order of magnitude higher than in cerebral cortex tissue. This fact must clearly be taken into future design considerations. In the rat cerebral cortex we also consistently observed drag (i.e. tension forces) during the phase where the electrodes were retracted from the brain. The drag forces were up to 6.2 times higher in cortical tissue. In the peripheral nerve data presented here, the drag force was much smaller than both the penetration and maximum force, indicating that advancing the electrode is by far more stressful for the electrode than retracting the electrode from the tissue. We speculate that the drag forces

are related to adhesion of the neural tissue to the electrode. The critical buckling force of a single-shaft *ACREO* electrode was calculated to be 1 mN – 4 mN, which was consistent with the experimentally measured break force (5.1 ± 2.1 mN). It was not possible to measure any break force for the tungsten electrode, i.e. the electrode would bend but not break when it was pushed against a hard surface. The theoretical bending moment analysis also showed that the strength of the *ACREO* electrode would be improved by a factor of 4 by increasing the thickness of the electrode by a factor of 2. Shortening the electrode by 5 mm would further improve the strength of the electrode by 50%. Assuming the mode of buckling is restricted to fixed-pivot buckling, these changes should increase the strength to approximately equal the tungsten electrode.

ACKNOWLEDGMENTS

Thanks to Peter Norlin, *ACREO* AB, Kista, Sweden for providing the *ACREO* electrodes. Thanks to the staff at Biomedicinsk Laboratorium, Aalborg Hospital for assistance during the animal experiment. This work was funded by EU grant IST-1999-10073.

REFERENCES

- [1] Hofmann UG, de Schutter E, de Curtis E, Yoshida K, Thomas U, and Norlin P, "On the Design of Multi-Site Microelectrodes for Neuronal Recordings," *Proc. MICRote*, vol. 1, pp. 283-288, 2000.
- [2] Hofmann UG, Folkers A, Malina T, Biella G, de Curtis E, de Schutter E, Yoshida K, Thomas U, Höhl D, and Norlin P, "Towards a Versatile System for Advanced Neuronal Recordings Using Silicon Multisite Electrodes," *Biomedizinische Technik*, vol. 45, no. E1, pp. 169-170, 2000.
- [3] Hofmann UG, Folkers A, Mosch F, Höhl D, Kindlundh M, and Norlin P, "A 64(128)-channel Multisite Neuronal Recording System," *Biomed Tech (Berl)*, vol. 47, no. Suppl 1 Pt 1, pp. 194-197, 2002.
- [4] Norlin P, Kindlundh M, Mouroux A, Yoshida K, Jensen W, and Hofmann UG, "A 32-site Neural Recording Probe Fabricated by Double Sided Deep Reactive Ion Etching of Silicon-on-Insulator Substrates," *Journal of Micromechanics and Microengineering*, 2001.
- [5] Yoshida K, Jensen W, Norlin P, Kindlundh M, and Hofmann UG, "Characterisation of Silicon Microelectrodes from the EU VSAMUEL Project," *Proceedings 35. Jahrestagung der Deutschen Gesellschaft für Biomedizinische Technik e. V. (DGMBT)*, 2001.
- [6] Jensen W, Yoshida K, Malina T, and Hofmann UG, "Measurement of Intrafascicular Insertion Force of a Tungsten Needle Into Peripheral Nerve," *23rd Annual International Conference of the IEEE-EMBS*, vol. 3, pp. 3108-3109, 2001.
- [7] Jensen W, Hofmann UG, and Yoshida K, "Assessment of Subdural Insertion Force of Single-Tine Microelectrodes in Rat Cerebral Cortex," *Proceedings of the 25th Annual International Conference of the IEEE*, vol. 3, pp. 2168-2171, 2003.
- [8] Biella G, Uva L, Hofmann UG, and de Curtis M, "Associative Interaction Within the Superficial Layers of the Entorhinal Cortex of the Guinea Pig," *J Neurophysiol*, vol. 88, pp. 1159-1165, 2002.
- [9] Volny-Luraghi A, Maex R, Vos B, and de Schutter E, "Peripheral Stimuli Excite Coronal Beams of Golgi Cells in Rat Cerebellar Cortex," *Neuroscience*, vol. 113, no. 2, pp. 363-373, 2002.
- [10] Biella G, Uva L, and de Curtis M, "Network Activity Evoked by Neocortical Stimulation in Area 36 of the Guinea Pig Perirhinal Cortex," *J Neurophysiol*, vol. 86, pp. 164-172, 2001.
- [11] Edell DJ, Toi VV, McNeil VM, and Clark LD, "Factors Influencing the Biocompatibility of Insertable Silicon Microshafts in Cerebral Cortex," *IEEE Trans Biomed Eng*, vol. 39, no. 6, pp. 635-643, 1992.
- [12] Najafi K and Hetke J, "Strength characterization of silicon microprobes in neurophysiological tissues," *IEEE Trans Biomed Eng*, vol. 37, no. 5, pp. 474-481, 1990.
- [13] Najafi K, Ji J, and Wise KD, "Scaling Limitation of Silicon Multichannel Recording Probes," *IEEE Trans Biomed Eng*, vol. 37, no. 1, pp. 1-11, 1990.
- [14] Portillo F, Mobley P, Moore J, and McCreery D, "Feasibility of a central nervous system auditory prosthesis: penetrating microelectrode insertion force studies," *Ann Otol Rhinol Laryngol Suppl*, vol. 166, pp. 31-33, 1995.
- [15] Howard MA, Abkes BA, Ollendieck MC, Noh MD, Ritter RC, and Gillies GT, "Measurement of the Force Required to Move a Neurosurgical Probe Through in vivo Human Brain Tissue," *IEEE Trans Biomed Eng*, vol. 46, no. 7, pp. 891-894, 1999.
- [16] Ritter RC, Quate EG, Gillies GT, Grady MS, Howard MA, and Broaddus WC, "Measurement of friction on straight catheters in in vitro brain and phantom material," *IEEE Trans Biomed Eng*, vol. 45, no. 4, pp. 476-485, 1998.